Primordial role of cobalt valence in the magnetotransport properties of oxygen deficient perovskites $Sr_{1-x}Ln_xCoO_{3-\delta}$

Primordial role of cobalt valence in the magnetotransport properties of oxygen deficient perovskites Sr$_{1-x}$Ln$_x$CoO$_{3-\delta}$

B Raveau[1], V Pralong, V Caignaert, M Hervieu and A Maignan

Laboratoire CRISMAT, UMR 6508 CNRS-EnsiCaen, 6 b^d Maréchal Juin, 14050 CAEN Cedex 1, France

E-mail: bernard.raveau@ensicaen.fr

Abstract

Oxygen deficient perovskite cobaltites Sr$_{1-x}$Ln$_x$CoO$_{3-\delta}$ ($x = 0.10, 0.20$) were studied, varying the nature of Ln from La to Ho. In these materials, whose oxygen deficiency and consequently cobalt valence, V_{Co}, vary continuously with the size of Ln^{3+}, it is shown that V_{Co} plays a primordial role in the magnetotransport properties. There indeed exists a crossover around $V_{Co} = +3.43$, below which the oxides are weakly ferromagnetic and semiconductors at low temperature, with a large magnitude of the negative magnetoresistance, up to -60% at 4.2 K, whereas above this valence the oxides are metallic ferromagnets. Moreover, the magnetoresistance increases importantly as V_{Co} decreases in the first region, whereas T_C increases with V_{Co} in the second one.

(Some figures in this article are in colour only in the electronic version)

1. Introduction

Soon after the discovery of colossal magnetoresistance in manganites [1, 2], cobaltites with a similar formulation, Sr$_x$Ln$_{1-x}$CoO$_{3-\delta}$, were found to exhibit large negative magnetoresistance for low values, i.e. $x < 0.30$ [3, 4]. In contrast, the Sr-rich side, $x = 1$, SrCoO$_3$, obtained under high oxygen pressure of more than 150 MPa [5, 6], was shown to be a ferromagnetic metal [7] without any significant magnetoresistance. Besides these stoichiometric cobaltites, oxygen deficient perovskites were synthesized, such as the brownmillerite-type phase SrCoO$_{2.5}$ [8, 9] obtained at normal oxygen pressure and the cobaltite SrCoO$_{2.75}$ [10] obtained by annealing the latter under an oxygen pressure of 15 MPa. On regarding their magnetic properties these two oxygen deficient perovskites were not found to be very attractive since the first one was found to be a paramagnetic semiconductor [7], whereas the second one was also shown to be weakly

---

[1] Author to whom any correspondence should be addressed.

magnetic and semiconducting with a very small positive magnetoresistance of only 0.5% in 7 T at 10 K [10]. The study of the chemically oxidized perovskite $Sr_{1-x}La_xCoO_{3-\delta}$ on the Sr-rich side, i.e. for x ranging from 0.10 to 0.50 [11], also showed the existence of large oxygen deficiency for the Sr-rich compositions ($x = 0.1$, 0.2), whereas beyond $x = 0.2$ the oxygen stoichiometry was found to be close to 'O$_3$'. The large increase of the magnetic susceptibility observed by these authors after chemical oxidation of the Sr-rich phases, $x \sim 0.1$–0.2, suggests that it should also be possible to induce transition from semiconducting antiferromagnet to metallic ferromagnet by tuning the oxygen deficiency in these oxides and thus to enhance the magnetoresistance properties. We have thus revisited the $Sr_{1-x}Ln_xCoO_{3-\delta}$ system for $x \leqslant 0.2$ and we have extended our investigations to the other lanthanides. In the present study of the oxygen deficient perovskites, $Sr_{0.9}Ln_{0.1}CoO_{3-\delta}$ and $Sr_{0.8}Ln_{0.2}CoO_{3-\delta}$, we show that the cobalt valence V_{Co} plays a primordial role in the magnetotransport properties of the latter, dividing the phase diagram into two regions corresponding to a metallic ferromagnet and a magnetoresistive semiconductor above and below a cobalt valence of 3.43 respectively. We also show that for the metallic ferromagnet ($V_{Co} > 3.43$) the Curie temperature increases with the cobalt valence from 140 to 229 K, at 4 K and in 7 T, whereas in the semiconductive weakly ferromagnetic region ($V_{Co} < 3.43$), the magnetoresistance effect increases as the cobalt valence decreases, from about -6% to about -60% at the same temperature.

2. Experimental section

2.1. Synthesis

All the samples of the $Sr_{0.9}Ln_{0.1}CoO_{3-\delta}$ and $Sr_{0.8}Ln_{0.2}CoO_{3-\delta}$ series with Ln = La, Pr, Nd, Sm, Eu, Gd, Tb, Dy were prepared in the same experimental conditions. The stoichiometric mixtures of Ln_2O_3 or Pr_6O_{11}, $SrCO_3$ and Co_3O_4 were first finely ground in an agate mortar and calcined at 800 °C in an oxygen flow in order to decompose the carbonate and favour the cobalt oxidation. The powders were then ground again, pressed in the form of parallepipedal bars $2 \times 2 \times 10$ mm^3 under 10^4 kg cm^{-2} and sintered at 1200 °C in an oxygen flow for 12 h.

Several of the above samples were annealed for 12 h either under an oxygen pressure of 100 bars at 400 °C, or in a nitrogen flow, or in an argon–hydrogen flow (H$_2$/5%) in order to test the effect of the oxygen stoichiometry upon the properties.

2.2. Chemical and physical characterization

X-ray diffraction (XRD) patterns were collected using a Philips diffractometer PW1710/1729 with Cu Kα ($\lambda = 0.154\,06$ nm) between 10° and 130° (2θ) with a step of 0.02° at room temperature. Rietveld refinement using FullProf [12] was performed on the pristine and oxidized phases. The electron diffraction study was carried out with a JEOL 200cx microscope, working at 200 kV. The cationic composition was determined by energy dispersive spectroscopy (EDS), using a Kevex analyser mounted on an HRTEM electron microscope. Iodometric and complexometric titrations were performed to determine the cobalt oxidation state in the prepared phases. For iodometric titration, the end-point was electrochemically determined by following the potential of the solution with platinum electrodes versus ECS electrode, while the current was held at zero. The sample (about 50 mg) was dissolved in a molar acetic buffer solution (about 50 ml) containing an excess of KI (about 1 g). Co^{3+} and Co^{4+} species were reduced to Co^{2+} together with formation of iodine species in stoichiometric amount. Iodine was therefore titrated with 0.1 N $Na_2S_2O_3$ solution using thiodene (starch) as colorimetric indicator in addition to the potential evolution. In order to have access to the

Table 1. Chemical and physical characterizations for the as-prepared $Sr_{0.9}Ln_{0.1}CoO_{3-\delta}$ and $Sr_{0.8}Ln_{0.2}CoO_{3-\delta}$. (Note: It., metallic; FM, ferromagnetic; SC, semiconductor; W, weak.)

	Cobalt oxidation state	Oxygen content	Mag. & cond.	T_C (K)	M (1.45 T)$_{5\ K}$ (μ_B/Co)	MR at 5 K (%)	ρ (Ω cm) at 5 K	Cell parameter a (Å)
				$Sr_{0.9}Ln_{0.1}CoO_{3-\delta}$				
La	3.53	2.81	It. FM	188.3	1.6	—	4×10^{-3}	3.842
Pr	3.56	2.83	It. FM	181	1.44	1	7×10^{-3}	3.836
Nd	3.53	2.82	It. FM	172.7	1.20	0.9	8.5×10^{-3}	3.837
Sm	3.49	2.79	It. FM	167.1	0.95	1.5	2×10^{-2}	3.839
Eu	3.43	2.77	SC FM	153.7	0.88	6	3×10^{-2}	3.836
Gd	3.36	2.73	SC FM	146.5	0.78	11	5×10^{-2}	3.837
Tb	3.34	2.72	SC FM	140	0.72	11	3×10^{-2}	3.840
				$Sr_{0.8}Ln_{0.2}CoO_{3-\delta}$				
La	3.56	2.88	It. FM	228.6	2.08	0	1×10^{-3}	3.836
Pr	3.55	2.87	It. FM	203	1.64	1	2.5×10^{-3}	3.830
Nd	3.48	2.84	It. FM	200	1.53	0.9	3×10^{-3}	3.828
Sm	3.29	2.75	SC W FM	164	0.40	7.5	4×10^{-2}	3.830
Gd	3.16	2.68	SC W FM	—	0.23	35	40	3.837
Tb	3.15	2.67	SC W FM	—	0.19	60	4×10^3	3.834

global amount of cobalt species in the sample, a complexometric titration was performed; 50 ml of H_2O and 7 ml NH_3 28% were added and titrated with EDTA 0.1 N using murexide as colorimetric indicator. Reproducibility for δ in parallel experiments is estimated to be 0.02. The oxygen content of some samples was also determined by thermogravimetric reduction in a dry 10% H_2/Ar mixture at 800 °C. The oxygen content, determined by TGA analysis, corresponds to the iodometric titration.

The magnetization data were collected in 1.45 T by means of a vibrating sample magnetometer after a zero-field cooling process. Resistivity values were obtained by using the four-probe technique on bars of typical dimensions 2 mm × 2 mm × 10 mm. Four indium contacts were ultrasonically deposited on the bars. Measurements of the resistance were made with a physical property measurement system (PPMS) from 5 to 400 K with magnetic field values up to 7 T.

3. Results and discussion

The x-ray powder patterns of these different samples were indexed in a cubic perovskite cell (table 1). Note therefore a very weak change in the cell parameter due to the opposite contribution of both earth rare element radius and oxygen content. The EDS analyses carried out on several tens of crystallites of the $Sr_{0.8}La_{0.2}CoO_{2.88}$ sample confirm the actual cation ratio, '$Sr_{0.8}La_{0.2}Co$', and the homogeneity of the sample $La_{0.2\pm0.03}Sr_{0.8\pm0.03}Co$ (calculated for one Co per formula unit). The reconstruction of the reciprocal space shows that two-thirds of the crystallites exhibit a simple perovskite cell (cubic or pseudo-cubic). This is shown by the $[100]_p$ and $[1\bar{1}1]_p$ in figures 1(a) and (b). The electron diffraction patterns of the other crystallites are characterized by the appearance of more or less intense extra reflections. A doubling of the c parameter, i.e. $2a_p$, is systematically observed in these complex supercells, often associated with diffuse streaks along c^*, generated by short range ordering (SRO) phenomena. The ED
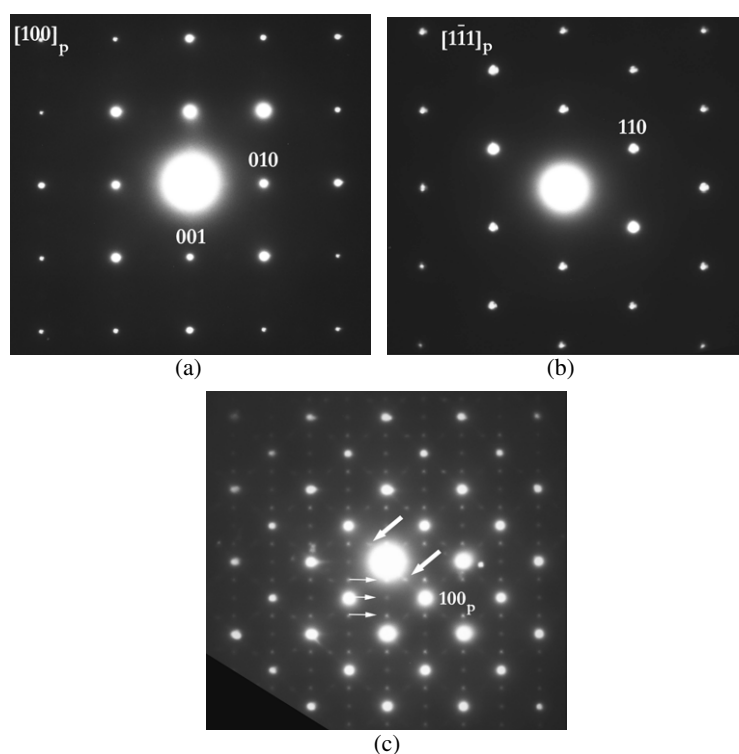
Figure 1. $Sr_{0.8}La_{0.2}CoO_{2.88}$ room temperature ED patterns along (a) $[100]_p$, (b) $[1\bar{1}1]_p$, and (c) ED pattern showing characteristic extra reflections of superstructure along c, where $a_p \times 2a_p$ (see large arrows), SRO and $2a_p\sqrt{2} \times 2a_p\sqrt{2}$ (see small arrows) systems are superimposed.

investigation shows that the superstructures are stabilized in the form of small or tiny twinning domains in the cubic matrix, leading to complex ED patterns, as illustrated in figure 1(c), where $a_p \times 2a_p$ (see large arrows in figure 1(c)), SRO and $2a_p\sqrt{2} \times 2a_p\sqrt{2}$ (see small arrows in figure 1(c)) systems are superimposed.

The iodometric titration shows that all these as-prepared perovskites are oxygen deficient. In each series, '$Sr_{0.9}Ln_{0.1}$' and '$Sr_{0.8}Ln_{0.2}$', the oxygen content and consequently the cobalt valency is closely related to the size of the lanthanide (table 1, figure 2). For the larger cations—La^{3+}, Pr^{3+} and Nd^{3+}—the cobalt valence does not vary a lot, ranging from +3.56 to 3.48, whereas beyond Nd^{3+}, i.e. from Sm^{3+} to Tb^{3+}, the cobalt valence decreases significantly with the size of the lanthanide, from +3.49 to 3.34 in the $Sr_{0.9}Ln_{0.1}$ series and from +3.29 to 3.15 in the '$Sr_{0.8}Ln_{0.2}$' series. The smaller valence of the second series compared to the first one confirms the size effect of the A-site cation upon the cobalt valence. Thus, the ability of oxygen to enter the perovskite lattice decreases with the average size of the A-site cation. For r_A ranging from 1.032 to 0.923 Å, this effect is more pronounced for the smaller cations ($r_A < 0.96$ Å).

The magnetization curves $M(T)$ registered under 1.45 T (figure 3) show that all the samples exhibit a ferromagnetic component. In both series, the magnetic moment at 5 K, $M_{5\,K}$, as well as the Curie temperature T_C, decrease as the size of the lanthanide cation decreases. Nevertheless, the '$Sr_{0.9}Ln_{0.1}$' and '$Sr_{0.8}Ln_{0.2}$' series behave differently: in the first one, $M_{5\,K}$ and T_C decrease fairly continuously from La^{3+} to Tb^{3+}, whereas in the second one there is a gap
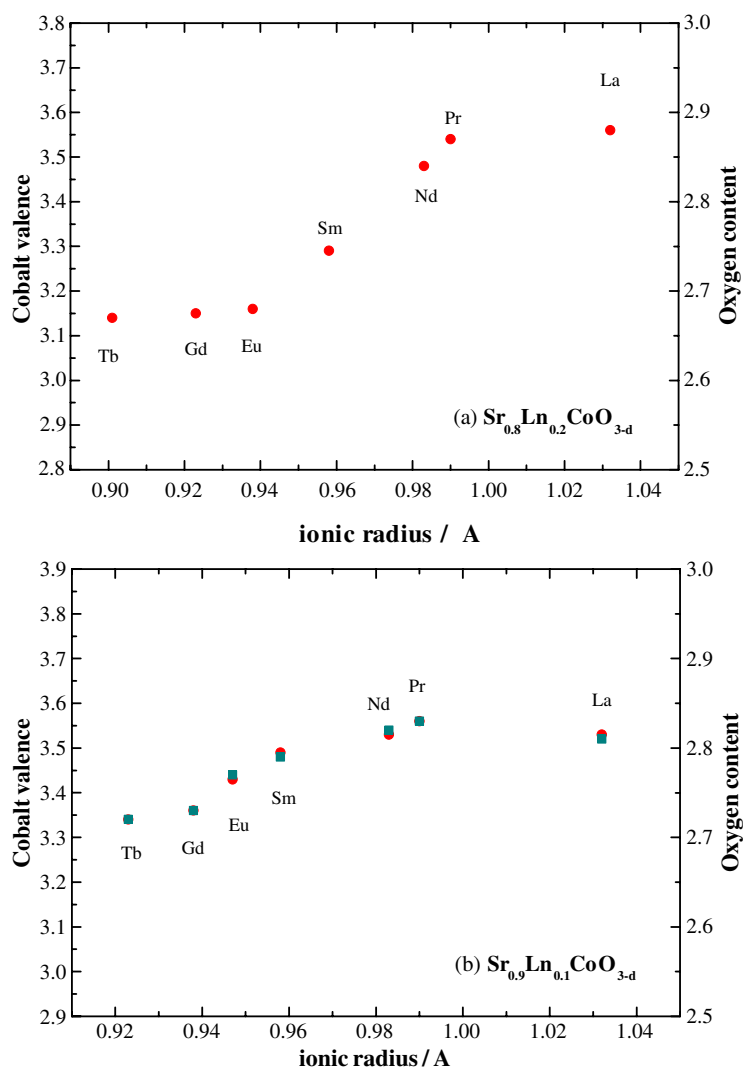
Figure 2. Evolution of the oxygen content (right y axis) or cobalt oxidation state (left y axis) versus ionic radius for (a) $Sr_{0.8}Ln_{0.2}CoO_{3-\delta}$ and (b) $Sr_{0.9}Ln_{0.1}CoO_{3-\delta}$.

between the oxides 'La, Pr, Nd' which are more ferromagnetic and the oxides 'Sm, Tb, Gd' which are labelled as weak ferromagnets. The enlargement of the $M(T)$ curves for Gd and Tb (inset figure 3(a)) reveals a small bump between 250 and 300 K. This could be related to the presence of antiferromagnetism as in $Sr_{2/3}Y_{1/3}CoO_{2.79}$ with $T_N = 320$ K [13]. Moreover, it is remarkable that the '$Sr_{0.8}Ln_{0.2}$' series exhibits higher T_C and $M_{5 K}$ than the '$Sr_{0.9}Ln_{0.1}$' series (table 1).

The study of the resistivity versus temperature demonstrates two different kinds of behaviour. The first one deals with the oxides $Sr_{0.9}Ln_{0.1}CoO_{3-\delta}$ with Ln = La, Pr, Nd, Sm and $Sr_{0.8}Ln_{0.2}CoO_{3-\delta}$ with Ln = La, Pr, Nd which exhibit a metal-like behaviour ($d\rho/dT > 0$) as shown for instance for $Pr_{0.1}Sr_{0.9}CoO_{2.83}$ (figure 4(a)) characterized by a metal to metal transition, whose transition temperature T_{M-M} coincides with T_C. Thus, all these perovskites
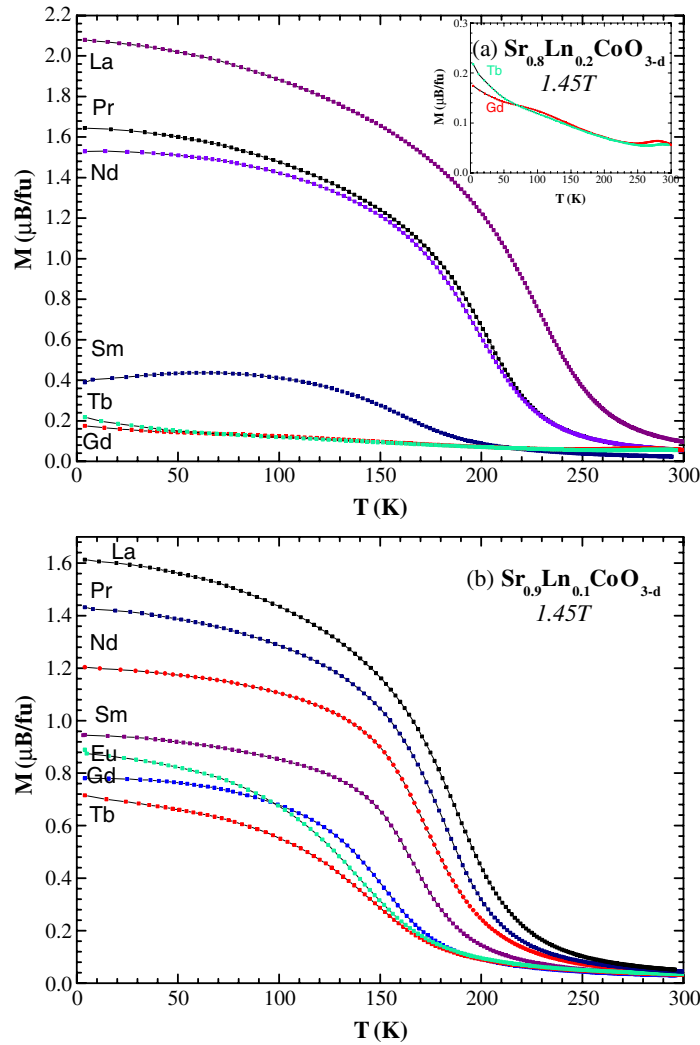
Figure 3. Magnetization curves $M(T)$ registered within 1.45 T for (a) $Sr_{0.8}Ln_{0.2}CoO_{3-\delta}$ Inset: enlargement curve for Ln = Gd, Tb and (b) $Sr_{0.9}Ln_{0.1}CoO_{3-\delta}$.

can be described as metallic ferromagnets below T_C and metallic paramagnets above T_C. This transition is similar to that previously observed in $SrCoO_3$ [7] and $SrRuO_3$ [14] and is usually explained by a reduction of the spin scattering as the ferromagnetic state appears. Note also that in each series, '$Sr_{0.9}Ln_{0.1}$' and '$Sr_{0.8}Ln_{0.2}$', the resistivity increases as the size of the lanthanide decreases (table 1), e.g. from $\sim 4 \times 10^{-3}$ Ω cm for Ln = La at 5 K to $\sim 2 \times 10^{-2}$ Ω cm for Ln = Sm in the first series and from 1×10^{-3} Ω cm for Ln = La to 3×10^{-3} Ω cm for Ln = Nd in the second series. The second type of behaviour is observed for smaller lanthanides, i.e. for Ln = Eu, Gd, Tb in the '$Sr_{0.9}Ln_{0.1}$' series and for Ln = Sm, Eu, Gd, Tb in the '$Sr_{0.8}Ln_{0.2}$' series. All these perovskites exhibit a negative $d\rho/dT$ coefficient as shown for example by $Sr_{0.8}Tb_{0.2}CoO_{2.67}$ (figure 4(b)). These two series differ by the order of magnitude of the resistivity: in the '$Sr_{0.9}Ln_{0.1}$' series, the resistivity values are rather low, ranging from 10^{-2} to 5×10^{-2} Ω cm, whereas in the '$Sr_{0.8}Ln_{0.2}$' series, much higher resistivity values are observed,
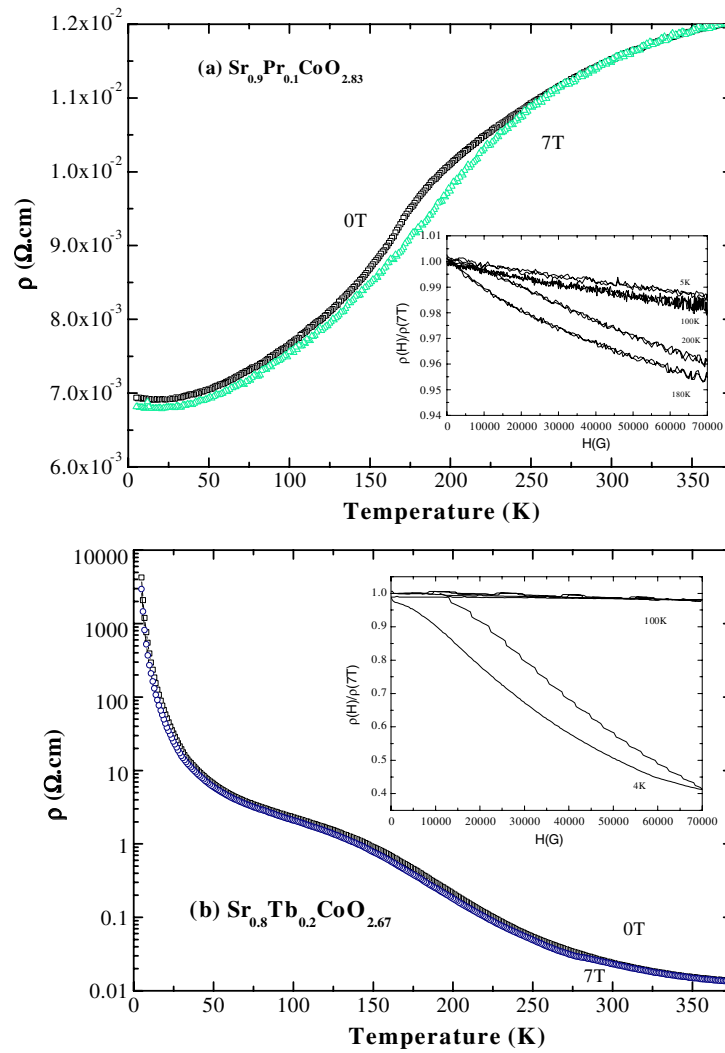
Figure 4. Thermal dependence of the resistivity $\rho(T)$ and inset, isothermal magnetic field (H) dependence $\rho(H)$, of the normalized resistivity for (a) $Pr_{0.1}Sr_{0.9}CoO_{2.83}$, and (b) $Tb_{0.2}Sr_{0.8}CoO_{2.67}$. 0 and 7 T refer to the external applied magnetic field values.

which increase dramatically from Sm to Tb (e.g. at 5 K from 4×10^{-2} Ω cm for Sm to 4×10^3 Ω cm for Tb).

The investigation of the magnetotransport properties of these cobaltites also allows two different kinds of behaviour to be distinguished. For the metallic ferromagnets one systematically observes that a very small negative magnetoresistance defined as $|\%MR| = 100 \times \frac{\rho_H - \rho_{H=0}}{\rho_{H=0}}$ occurs in the vicinity of T_C but it remains low in absolute value, i.e. smaller than 5% in 7 T. This is illustrated by the $\rho(T)$ and $\rho(H)$ curves of the oxide $Sr_{0.9}Pr_{0.1}CoO_{2.83}$ (inset figure 4(a)) for which the $|\%MR|$ value at 5 K in 7 T is smaller than 1%, reaching a maximum of 4.5% at $T_C = 180$ K. In contrast, for the sample characterized by $d\rho/dT < 0$ coefficients, high $|\%MR|$ values can be reached (table 1) and the latter are maximum at 5 K, decreasing progressively as the temperature increases. This is illustrated by the $\rho(T)$ and
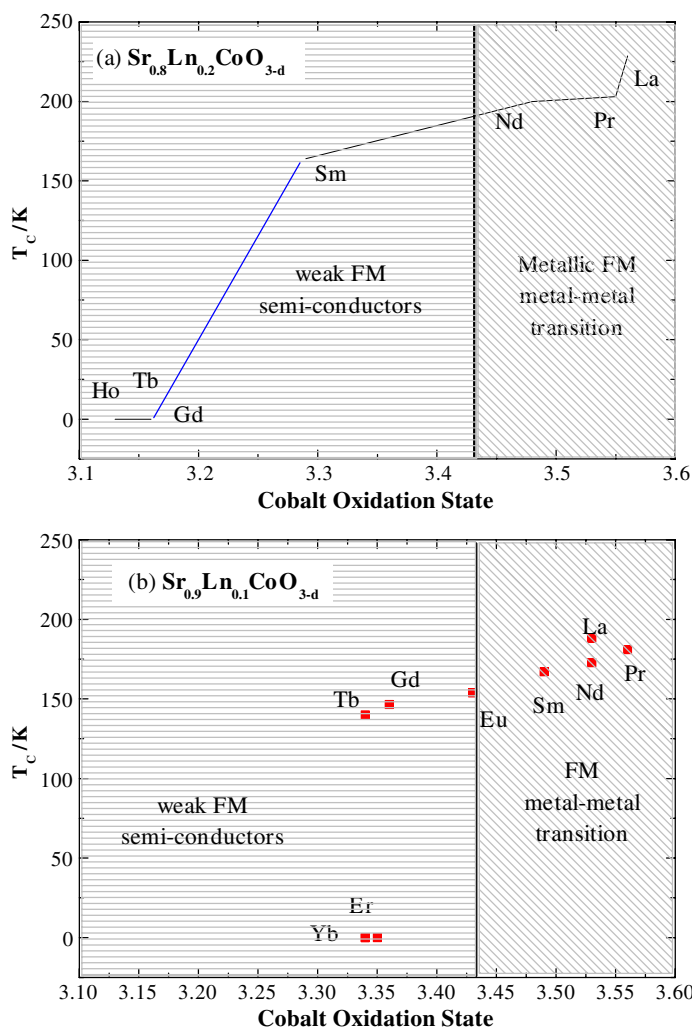
Figure 5. Curie temperature T_C evolution versus the cobalt valence for (a) $Sr_{0.9}Ln_{0.1}CoO_{3-\delta}$ and (b) $Sr_{0.8}Ln_{0.2}CoO_{3-\delta}$.

$\rho(H)$ curves of the oxide $Sr_{0.8}Tb_{0.2}CoO_{2.67}$ (inset figure 4(b)) for which the $|\%MR|$ value at 5 K reaches 60%, but decreases rapidly as T increases, being already negligible at 100 K.

These two sorts of behaviour, observed for the magnetic and transport properties of these Sr-rich cobaltites and especially for their magnetoresistance properties, show a great similarity with those previously observed in the stoichiometric system $Sr_{1-x}La_xCoO_3$ by Wu *et al* [15] and by Senaris-Rodriguez *et al* [16] for much larger x values ($x > 0.40$). The first series of cobaltites indeed exhibit a metallic behaviour, similar to that observed by the previous authors [15, 16] for $Sr_{0.45}La_{0.55}CoO_3$, and importantly their MR reaches a maximum near T_C as for this oxide. Thus, it can be assumed, as proposed by the authors, that these metallic ferromagnets exhibit, like manganites, a true double-exchange effect. The second series of cobaltites, which are semiconducting weak ferromagnets, is comparable to La-rich cobaltites $Sr_{1-x}La_xCoO_3$ ($x > 0.75$), leading for the $\rho(T)$ curve of $Sr_{0.9}Eu_{0.1}CoO_{2.77}$ to a re-entrant
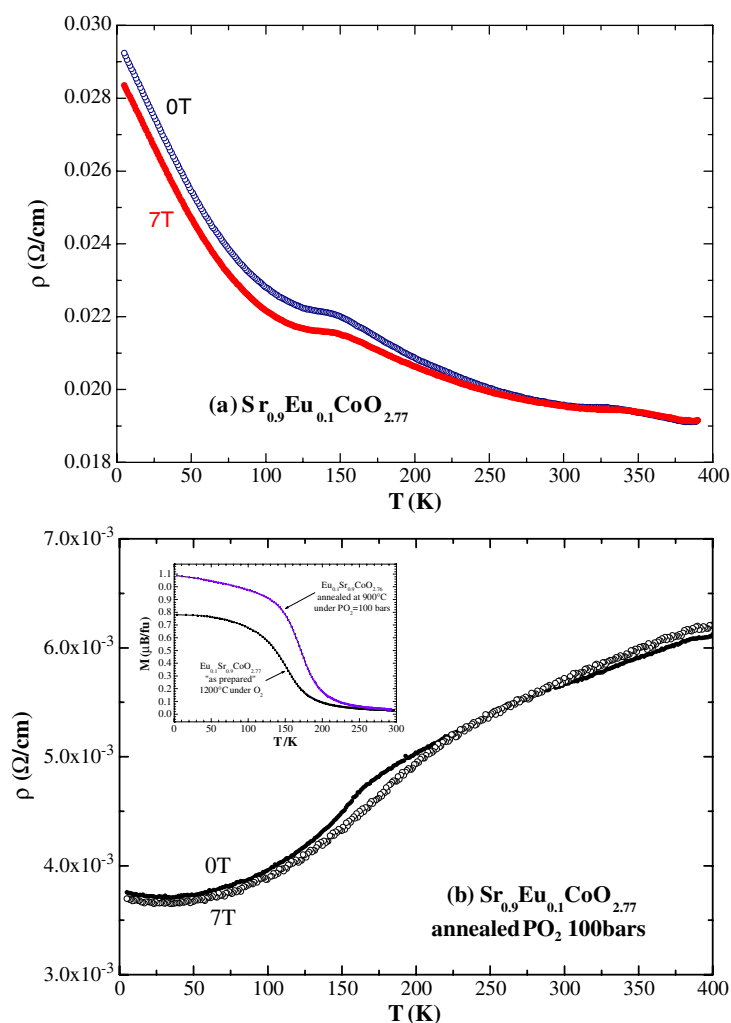
Figure 6. Thermal dependence of the resistivity $\rho(T)$ for $Eu_{0.1}Sr_{0.9}CoO_{3-\delta}$ as prepared (a) and after $P_{O_2} = 100$ bars annealing (inset: corresponding $M(T)$ curves) (b).

transition similar to that obtained by Senaris-Rodriguez *et al* [16] for $La_{0.8}Sr_{0.2}CoO_3$. This upturn of the resistance at low temperature was also observed by Wu *et al* [15] for a similar lanthanum composition. This effect can be interpreted, in agreement with these authors, either as a re-entrant insulator to metal transition or as a weak localization. The extremely high value of the MR in these weak ferromagnets, which reaches a maximum at 4.2 K, is also similar to that previously observed for $La_{0.8}Sr_{0.2}CoO_3$. It may be due, as proposed by Wu *et al* [15], to spin-dependent effects, which originate from the alignment of the spins in a high magnetic field.

Thus, the above comparisons show that oxides with almost 'symmetric' cationic compositions can exhibit rather close magneto-transport properties. This suggests that the oxygen stoichiometry of these perovskites plays a major role in their properties. The behaviour of these two series of cobaltites can indeed be understood by considering the evolution of their properties versus the cobalt valence (figure 5). The phase diagram obtained for the
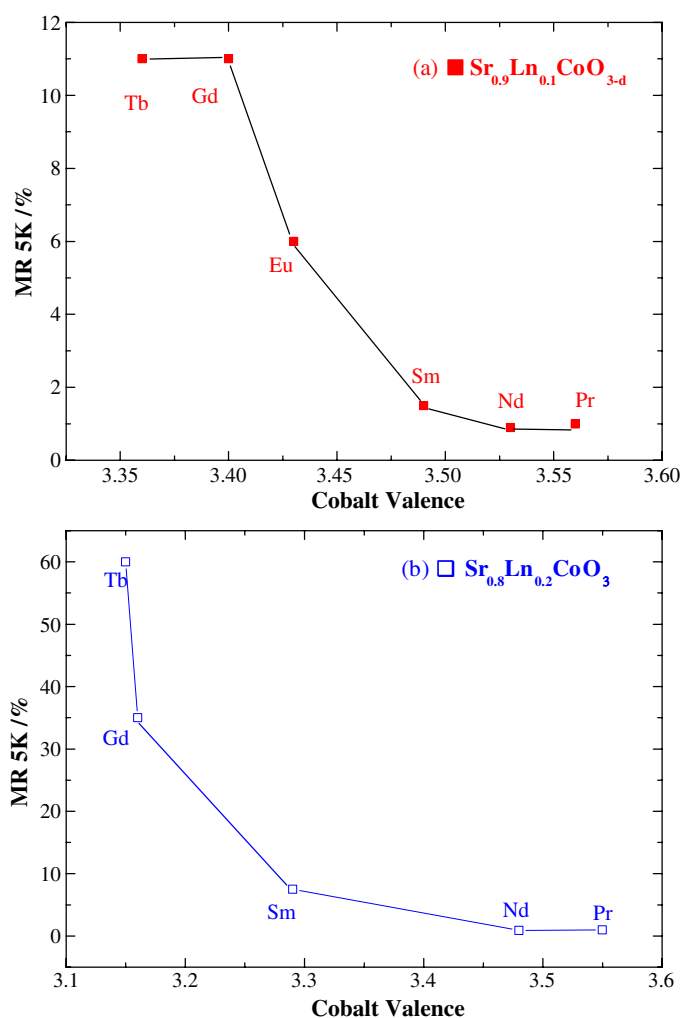
Figure 7. Evolution of the magneto-resistance at 5 K, $|\%MR| = 100 \times \frac{\rho_{H} - \rho_{H=0}}{\rho_{H=0}}$ versus the cobalt valence for the (a) $Sr_{0.9}Ln_{0.1}CoO_{3-\delta}$ and (b) $Sr_{0.8}Ln_{0.2}CoO_{3-\delta}$ series.

$Sr_{0.9}Ln_{0.1}CoO_{3-\delta}$ series (figure 5(a)) clearly shows that there exist two different regions, depending on the cobalt valence: for $V_{Co} > +3.43$ the cobaltites exhibit a metal-like behaviour whatever the temperature, whereas for $V_{Co} < +3.43$ they exhibit a semiconducting behaviour. The oxide $Sr_{0.9}Eu_{0.1}O_{2.77}$, located at the limit ($V_{Co} = +3.43$), although it exhibits a low resistivity ($\rho \sim 2 \times 10^{-2}$ Ω cm), is semiconductor-like but shows a re-entrant transition between two different conducting states (figure 6(a)). Remarkably, its annealing under an oxygen pressure of 100 bars leads to a metallic behaviour (figure 6(b)) and to a significant increase of ferromagnetism (inset figure 6(b)). The chemical titration does not detect any variation of the oxygen content, suggesting that a very tiny increase of the cobalt valence is sufficient to switch the behaviour of this oxide. In the complete '$Sr_{0.9}Ln_{0.1}$' series, the Curie temperature increases smoothly as the cobalt valency increases from about 150 to 175 K, and the magnetic moment measured at 4.2 K increases continuously as the cobalt valency increases, except for the lanthanum cobaltite, which exhibits a slightly higher moment
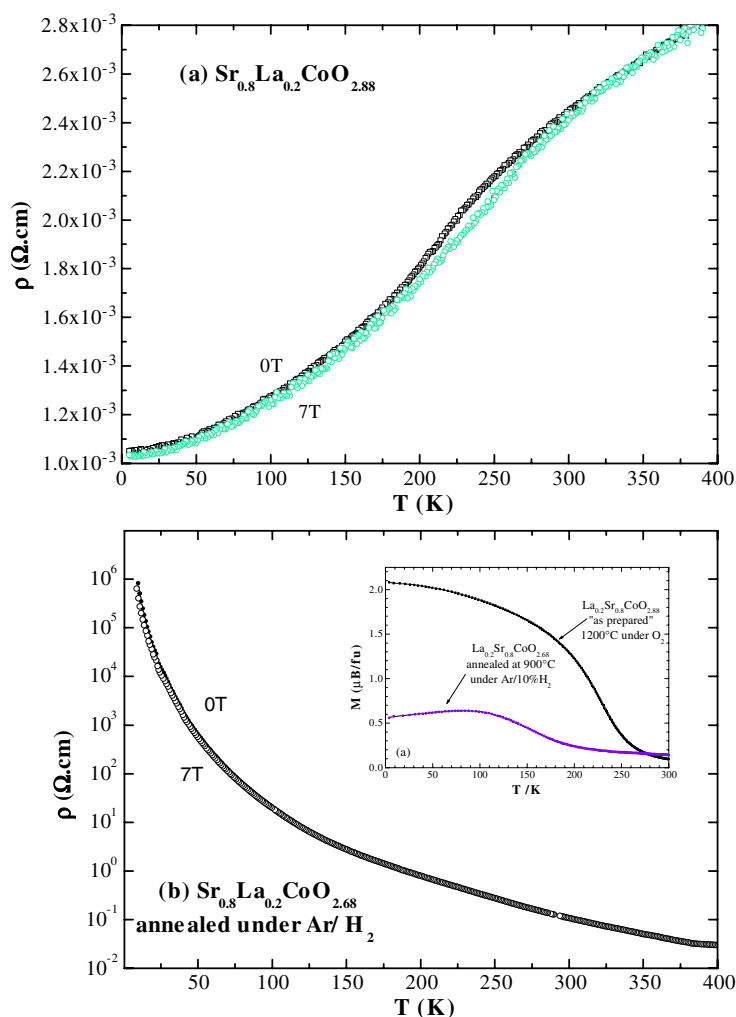
Figure 8. Thermal dependence of the resistivity $\rho(T)$ for $Sr_{0.8}Ln_{0.2}CoO_{3-\delta}$ (a) before and (b) after Ar/H$_2$ annealing. Inset: magnetization curves $M(T)$ registered at 1.45 T for $Sr_{0.8}Ln_{0.2}CoO_{3-\delta}$ before and after Ar/H$_2$ annealing.

than the neodymium and praseodymium phases in spite of its smaller or nearly equal cobalt valence. Thus, below T_C the cobaltites with $V_{Co} \leqslant 3.43$ are semiconductor-like and weakly ferromagnetic, whereas those with $V_{Co} > +3.43$ are metallic ferromagnets and exhibit a metal–metal transition leading to metallic paramagnets above T_C. These results show that the cobalt valence plays a prominent role in the magnetic and transport properties of these cobaltites. Nevertheless, the size of lanthanide cation may also have a minor influence on their properties, explaining that lanthanum, due to its larger size, may compensate the effects of lower valence of cobalt, by favouring the overlapping of the orbitals along the Co–O–Co bonds. The evolution of the magnetoresistance at 5 K in this series is also of great interest. One indeed observes that for $V_{Co} > +3.43$, in the ferromagnetic metallic state, the magnetoresistance at 5 K is very small (smaller than 2%) and does not vary with the cobalt valence, as expected for a bad metal, whereas, in contrast, a small jump of the MR

to 6% is observed just at the boundary between the two regions, i.e. at $V_{Co} = +3.43$. Then the magnetoresistance $|\%MR|$ increases significantly as V_{Co} decreases, and correlatively the resistivity increases (figure 7(a)). A rather similar behaviour is observed for the $Sr_{0.8}Ln_{0.2}Co_{3-\delta}$ series (figure 7(b)), except that in the latter case the cobalt valence decreases more rapidly with the ionic radius of Ln^{3+}, so that it is difficult to establish an accurate phase diagram. Nevertheless, it clearly appears that all the compositions with $V_{Co} \geqslant +3.43$ (La, Pr, Nd) are metallic ferromagnets /metallic paramagnets, characterized by a metal to metal transition at T_C, whereas for $V_{Co} < +3.43$ (Sm, Gd, Tb, Dy, Ho) the compounds exhibit a low magnetic moment at 5 K compared to the first ones and are semiconducting-like, so that they can be described as weak ferromagnetic semiconductors, or canted antiferromagnets. Remarkably, the evolution of the magnetoresistance in the '$Sr_{0.8}Ln_{0.2}$' series is very similar to that observed for the '$Sr_{0.9}Ln_{0.1}$' series: the metallic ferromagnets ($V_{Co} > +3.43$) are weakly magnetoresistive ($|\%MR| < 1\%$ at 5 K), whereas the weak ferromagnets ($V_{Co} < +3.43$) exhibit a rapid increase of their magnetoresistance from 7.5% to 70% at 5 K as the cobalt valence decreases from 3.29 (Sm) to 3.1 (Ho). The annealing of the metallic ferromagnet $Sr_{0.8}La_{0.2}CoO_{2.88}$ under Ar/H_2, which leads to a drastic decrease of the oxygen content of this phase to $Sr_{0.8}La_{0.2}CoO_{2.68}$ ($V_{Co} = +3.17$) confirms the important role of cobalt valence. The latter oxide becomes a semiconductor (figure 8) and exhibits a spectacular decrease of its ferromagnetic moment from 2.1 to 0.6 μ_B (inset figure 8). Finally, it is quite remarkable that the La-rich oxides $Sr_{0.45}La_{0.55}CoO_3$ and $La_{0.8}Sr_{0.2}CoO_3$ previously studied [15, 16], which seem to exhibit an 'O_3' stoichiometry, are metallic and semiconductive, respectively, in perfect agreement with the expected valence of cobalt in these oxides, +3.45 and +3.2, confirming the primordial role of cobalt valence in the magnetotransport properties of these cobaltites.

In conclusion, this study of the oxygen deficient perovskite cobaltites $Sr_{1-x}Ln_xCoO_{3-\delta}$ shows that the oxygen deficiency, and consequently the cobalt valence, primarily governed by the size of the A site cations, plays a prominent role in the magnetotransport properties of these materials. It demonstrates that a crossover between the ferromagnetic metallic state and the weak ferromagnetic semiconducting state appears for a particular valence of cobalt around $V_{Co} \approx 3.43$. Remarkably, for each domain, the magnetotransport properties are very sensitive to the cobalt valence: T_C indeed increases significantly with V_{Co} in the ferromagnetic metallic region, whereas the magnetoresistance at 5 K shows a large increase as V_{Co} decreases in the weak ferromagnetic semiconducting region. Clearly, the detailed study of the physics of these cobaltites will require a very accurate knowledge and control of their oxygen stoichiometry.

References

[1] Von Helmolt R, Holzapfel B, Schultz L and Samwer K 1994 *Phys. Rev. Lett.* **71** 2331
[2] Caignaert V, Maignan A and Raveau B 1995 *Solid State Commun.* **95** 357
[3] Mahendiran R, Raychaudhuri A K, Chaimini A and Sarma D D 1995 *J. Phys.: Condens. Matter* **7** L561
[4] Briceno G, Chang H, Sun X, Schultz P G and Xiang X D 1995 *Science* **270** 273
[5] Taguchi H, Shimada M and Koizumi M 1979 *J. Solid State Chem.* **29** 21
[6] Shaplygin I S and Lazarev V B 1985 *Russ. J. Inorg. Chem.* **30** 1828
[7] Bezdicka P, Wattiaux A, Grenier J C, Pouchard M and Hagermuller P 1993 *Z. Anorg. Allg. Chem.* **619** 7
[8] Takeda T, Yamaguchi Y and Watanabe H 1972 *J. Phys. Soc. Japan* **33** 970
[9] Takeda T, Kanno R, Takada T, Yamamoto O, Takano M and Bando Y 1986 *Z. Anorg. Allg. Chem.* **540** 259
[10] Maignan A, Martin C, Nguyen N and Raveau B 2001 *Solid State Sci.* **3** 57
[11] Sunstrom J E, Kamanujachary K V, Greenblatt M and Croft M 1998 *J. Solid State Chem.* **139** 388
[12] Rodriguez-Carvajal J 1990 *Collected Abstracts of Powder Diffraction Meeting (Toulouse, France)* p 127
[13] Goosens D J, Wilson K F, James M, Studer A J and Wang X L 2004 *Phys. Rev.* B **69** 134411
[14] Longo J M, Raccah P M and Goodenough J B 1968 *J. Appl. Phys.* **39** 1327
[15] Wu J and Leighton C 2003 *Phys. Rev.* B **67** 174408
[16] Senaris-Rodriguez M A and Goodenough J B 1995 *J. Solid State Chem.* **118** 323